2026 European Conference on Computing in Construction
Corfu, Greece
July 12-15, 2026

A DATA-DRIVEN KOOPMAN-MPC FOR MULTI-ACTUATOR AHU CONTROL

Youssef Elomari[1], Mustapha Habib[1], and Qian Wang[1,2]
[1]Division of Building Technology and Design, Department of Civil and Architectural Engineering, KTH Royal Institute of Technology, 114 28, Stockholm, Sweden
[2]Uponor AB, Hackstavägen 1, Västerås, 721 32, Sweden

Abstract

Air-handling units (AHUs) are major energy consumers in HVAC systems due to their coupled actuators and constrained multi-input multi-output operation. This paper proposes a data-driven Koopman-MPC framework that identifies lifted linear dynamics from building management system (BMS) data using EDMDc, enabling constrained MPC design for nonlinear AHU behavior. The approach is validated on a residential AHU in Stockholm, Sweden. Results demonstrate the feasibility of deploying Koopman-based predictive control using operational data, and a BMS-integrated edge implementation workflow is presented for practical building applications.

Introduction

In recent years, data-driven methods have become increasingly important for the operation and optimization of heating, ventilation, and air conditioning (HVAC) systems (Afram and Janabi-Sharifi, 2014). Air-handling units (AHUs) represent a critical component of building HVAC systems, responsible for conditioning and distributing air throughout building zones. Modern AHUs incorporate multiple actuators, including supply and return fans, mixing dampers, heating and cooling coils, and humidifiers, creating a complex multi-input multi-output (MIMO) control problem (Afram and Janabi-Sharifi, 2014; Matetić et al., 2022). Coordinating these actuators to achieve multiple objectives—energy efficiency, thermal comfort, indoor air quality poses significant challenges for conventional control approaches (Yue et al., 2023). Despite this multivariable and constrained nature, AHU control in many buildings still relies on decentralized proportional–integral–derivative (PID) and rule-based controllers implemented in the building management system (BMS) (Zou, Yu and Ergan, 2020). These strategies are robust and easy to commission, but they do not coordinate multiple actuators or explicitly handle constraints. At the same time, the increasing availability of high-resolution BMS data has accelerated progress in data-driven control methods. Most of the literature has focused on fault detection and diagnosis and on supervisory energy management and operational decision-making at scale (Deshmukh, Glicksman and Norford, 2020; Taheri et al., 2021; Matetić et al., 2022).Several studies have attempted to address AHU optimal control using data-driven methods. Optimization-based approaches using simplified models have been demonstrated for AHU regulation in simulation environments, often relying on reduced polynomial structures that cannot represent all internal AHU interactions(Zou, Yu and Ergan, 2020). Learning-based control has also been explored through deep reinforcement learning trained on operational datasets, reporting improvements relative to baseline operation while maintaining predicted discomfort around 10% using an LSTM-based surrogate (Zou, Yu and Ergan, 2020). Neural-network predictive controllers based on dynamic recurrent models have reported up to 69.9% energy reduction on historical data, while also indicating that nonlinear predictors inside the controller (Asvadi-Kermani et al., 2022). (Zheng, Wang and Wang, 2024) conducted a systematic comparison of model-based and data-driven economic MPC using the BOPTEST framework. Their results showed that data-driven methods achieved energy cost reductions within 5–10% Overall, the literature suggests that data-driven control can deliver substantial gains. However, robust AHU optimal control remains challenging due to nonlinear multivariable dynamics.

Koopman operator theory provides a promising route to address these challenges by representing nonlinear dynamics through linear evolution in a lifted space of observables (Wahba et al., 2023). The lifting map captures the nonlinear structure, while prediction evolves linearly in lifted coordinates, enabling the use of standard linear MPC solvers with explicit constraints. A finite-dimensional approximation of the Koopman operator can be learned directly from operational data using extended dynamic mode decomposition with control (EDMDc), which estimates lifted linear dynamics from measured state–input snapshot pairs (Zawacki and Abed, 2023).

In this paper, we develop a Koopman–MPC framework for coordinated multi-input supervisory control of an AHU using operational BMS data from the KTH Live-In Lab. We identify the Koopman predictor via EDMDc, embed the lifted linear dynamics into an MPC formulation, and regulate supply air temperature and exhaust airflow under actuator constraints. Closed-loop performance is evaluated using a high-fidelity model trained on measured data. We also present an edge implementation workflow compatible with BMS-integrated operation

Methodology

This section presents a Koopman–MPC framework for coordinated multi-input control of an air-handling unit (AHU). A finite-dimensional approximation of the Koopman operator is identified from operational building management system (BMS) data using extended dynamic mode decomposition with control (EDMDc). Closed-loop performance is evaluated using a high-fidelity neural state-space (NSS) surrogate model trained on measured data. Figure 1 summarizes the overall architecture and data flow.

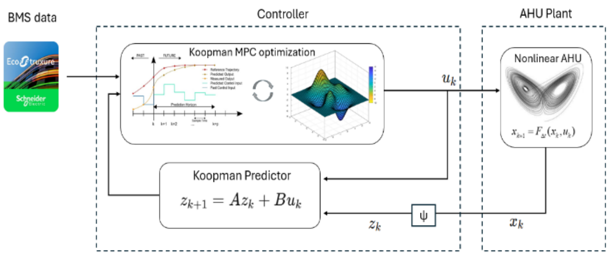

Figure 1: Overview of the proposed Koopman–MPC architecture

System definitions

The AHU is modeled as a nonlinear discrete-time system sampled at interval Δt

$$x_{k+1} = F_{\Delta t}(x_k, u_k)$$

where x_k denotes the system state and u_k the control input at time step k and Δt corresponds to the BMS sampling interval.

Based on available BMS measurements, the state and input vectors are defined as

$$x_k = \begin{bmatrix} T_{\mathrm{sup},k} & F_{\mathrm{sup},k} & T_{\mathrm{rec},k} & T_{\mathrm{exh},k} & F_{\mathrm{exh},k} \end{bmatrix}^{\top}$$

$$u_k = \begin{bmatrix} V_{\mathrm{heat},k} & T_{\mathrm{heat},k} & S_{\mathrm{sup},k} & S_{\mathrm{wheel},k} & S_{\mathrm{exh},k} \end{bmatrix}^{\top}$$

The control objective focuses on regulating supply air temperature and exhaust airflow, which are defined as the controlled outputs

$$y_k = \begin{bmatrix} T_{\mathrm{sup},k} \\ F_{\mathrm{exh},k} \end{bmatrix}$$

These variables directly affect indoor comfort and energy use and are therefore selected as the primary control targets. This multi-input setup matches the practical control objective. The controller adjusts the heating coil, fans, and heat-recovery wheel in a coordinated way rather than relying on a single actuator.

Koopman-based predictor for MPC

Koopman theory represents nonlinear state evolution through linear evolution of observable functions. For a discrete-time system, the Koopman operator $K_{\Delta t}$ acts on an observable g as

$$(K_{\Delta t} g)(x_k, u_k) = g\big(F_{\Delta t}(x_k, u_k)\big)$$

A practical predictor requires a finite-dimensional approximation. Following the EDMD framework, we select a dictionary of basis functions and project the Koopman operator onto its span.

We define a lifting map ψ that maps the normalized state into a higher-dimensional feature vector

$$z_k = \psi(x_k)$$

where ψ consists of polynomial basis functions selected to capture dominant nonlinearities observed in the data. The lifting map uses normalized measured states and a second-order polynomial dictionary with linear, squared, and pairwise interaction terms. All variables are normalized using the training-data mean and standard deviation. For five measured states, this gives a lifted-state dimension of 21 including the constant term.Using EDMDc, the lifted dynamics are approximated by the linear controlled system

$$z_{k+1} = Az_k + Bu_k$$

$$y_k \approx Cz_k$$

Where matrices A and B describe the evolution of the lifted state under the influence of the control inputs, while C maps the lifted coordinates back to the physical outputs.

To identify the Koopman system matrices, snapshot pairs are constructed from the operational dataset

$$Z = \begin{bmatrix} z_1 & \cdots & z_{N-1} \end{bmatrix}, Z^{+} = \begin{bmatrix} z_2 & \cdots & z_N \end{bmatrix}$$

$$U = \begin{bmatrix} u_1 & \cdots & u_{N-1} \end{bmatrix}$$

The lifted system matrices are obtained by solving a regularized least-squares problem

$$\min_{A,B} \left\| Z^{+} - \begin{bmatrix} A & B \end{bmatrix} \begin{bmatrix} Z \\ U \end{bmatrix} \right\|_F^2 + \lambda \left\| \begin{bmatrix} A & B \end{bmatrix} \right\|_F^2$$

Koopman-MPC formulation

At each control step k, MPC optimizes a sequence of future control inputs over a finite horizon. The Koopman–MPC optimization problem is formulated as

$$\min_{\{u_{k+i|k}\}_{i=1}^{N_p}} \sum_{i=1}^{N_p} \Big[(y_{k+i|k} - y_{r,k+i})^{\top} Q (y_{k+i|k} - y_{r,k+i}) + (u_{k+i|k} - u_{k+i-1|k})^{\top} R (u_{k+i|k} - u_{k+i-1|k}) \Big]$$

Where $y_{r,k+i}$ denotes the reference trajectory for supply air temperature and exhaust airflow. The first term penalizes tracking error, while the second term penalizes aggressive variations in the control inputs.

The optimization is subject to actuator magnitude and rate constraints

$$u_{\min} \le u_{k+i|k} \le u_{\max}$$

$$\Delta u_{\min} \le u_{k+i|k} - u_{k+i-1|k} \le \Delta u_{\max}$$

The Koopman–MPC uses a 15 min sampling time and a prediction horizon of 4 steps. The optimization is solved using sequential quadratic programming (SQP). Following our earlier AHU MPC setup on the same testbed, the baseline weighting is set to $Q = 1$and $R = 10^{-5}[1,1,1,1,1]$.

High-fidelity AHU model

To evaluate the Koopman-MPC under realistic conditions, a neural state-space (NSS) model is used as a high-fidelity surrogate of the AHU dynamics

$$x_{k+1} = f_\theta(x_k, u_k),\ y_k = h_\theta(x_k)$$

where f_θ and h_θ are nonlinear mappings parameterized by neural network weights θ. The NSS model is trained using one-step-ahead prediction on one year of measured BMS data with a 15-minute sampling resolution.
The NSS model is used solely for closed-loop performance evaluation and benchmarking and is not employed for prediction or control within the Koopman–MPC framework.

Case study

The proposed Koopman–MPC framework is evaluated on an AHU installed at the KTH Live-In Lab. The system serves four student apartments and consists of a rotary heat exchanger, variable-speed supply and exhaust fans, and a water-based heating coil, as illustrated in Figure 2.
Historical operational data were collected from the building management system (BMS) at a 15-minute resolution over three years. The dataset includes supply and exhaust air temperatures, airflow rates, heating-coil rate and temperature, fan speeds, and wheel speed. These measurements are used to identify the EDMDc Koopman predictor and to train the NSS surrogate model.

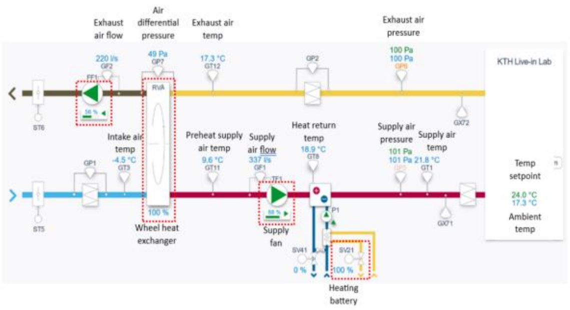

Figure 2: SCADA view of the AHU installed at the KTH Live-In Lab, illustrating the rotary heat exchanger, heating coil, and variable-speed supply and exhaust fans. The highlighted components correspond to the actuators considered in the proposed Koopman–MPC framework

Results

This section presents the results obtained using the proposed Koopman–MPC framework applied to the real AHU system use case described in Section 2. The analysis focuses on validating the high-fidelity neural state-space (NSS) model used as a surrogate plant, evaluating the predictive capability of the EDMDc-based Koopman linear predictor, and assessing the closed-loop performance of the MPC controller under realistic operating constraints.
The predictive accuracy of the NSS model was first assessed to ensure that it provides a reliable reference for closed-loop controller evaluation. The model was trained using one-step-ahead prediction on historical BMS data with a 15-minute sampling interval and validated on unseen data segments covering a wide range of airflow rates, heat-recovery operating points, and heating-coil conditions. Figure 3 compares measured and simulated air-temperature trajectories for the supply, recycled, and exhaust air streams. Minor deviations between measured and simulated signals are primarily observed during periods of rapid airflow variation, where sensor dynamics and short-term turbulence effects introduce additional uncertainty. Despite these effects, the overall agreement remains strong. The mean absolute error for supply-air temperature remains below 0.5 °C, while exhaust airflow prediction errors stay within 5 % over the validation period. These results confirm that the NSS model accurately represents the nonlinear behavior of the full-scale AHU and can be used as a high-fidelity surrogate plant for evaluating the proposed Koopman–MPC strategy.

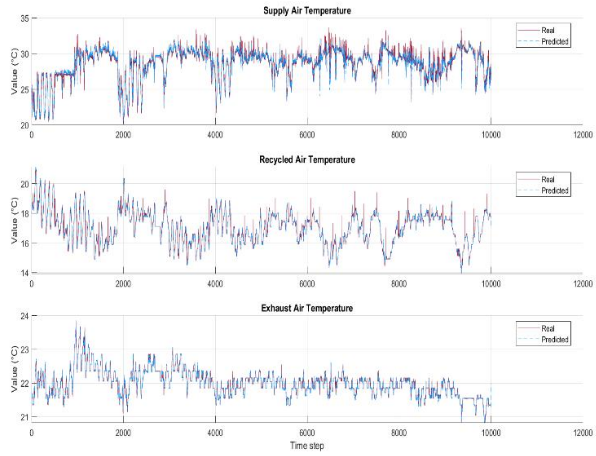

Figure 3: Comparison between measured and NSS-simulated air temperatures (supply, recycled, and exhaust) used for model validation

The multi-step prediction capability of the Koopman-based linear model identified via EDMDc was then evaluated. The lifted predictor is embedded in the MPC to forecast future temperature and airflow trajectories over the prediction horizon. The results show that the Koopman model maintains stable and physically consistent predictions despite the strong nonlinear coupling between airflow, heat recovery, and heating-coil operation. In particular, the predictor accurately captures the influence of airflow modulation on supply-air temperature, which is critical for coordinated multi-input control. As expected, prediction errors increase gradually with horizon length; however, they remain sufficiently small to support reliable MPC optimization.
Figure 4 illustrates the system response during a representative winter operating sequence. The controller successfully maintains both the supply-air temperature and supply airflow close to their respective setpoints while coordinating the heating coil, supply fan, exhaust fan, and rotary heat-exchanger speed. The MPC dynamically adjusts actuator combinations in response to disturbances and load variations, ensuring stable operation without violating actuator magnitude or rate

constraints.

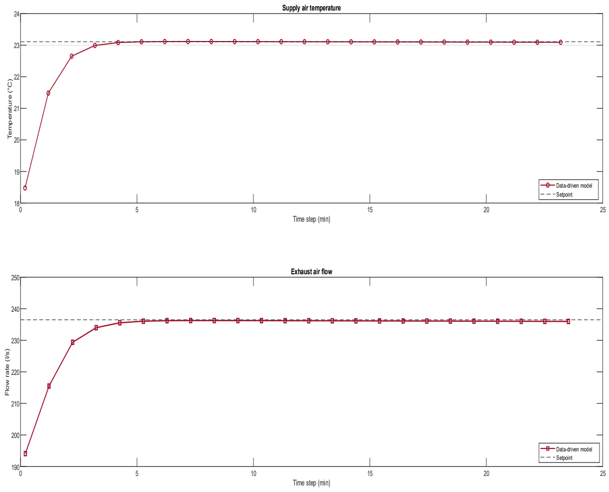

Figure 4:Closed-loop Koopman–MPC response showing supply-air temperature tracking and exhaust-airflow regulation during frost-risk conditions

Technical deployment consideration and edge implementation workflow

This section discusses the technical considerations for deploying the proposed Koopman–MPC framework within a building management system (BMS) using an edge computing architecture. While the control strategy is evaluated in a co-simulation environment in this work, the deployment design is presented to demonstrate practical feasibility and compatibility with existing industrial automation infrastructure.

BMS-integrated edge architectures

The proposed Koopman–MPC framework is designed to operate within a BMS-integrated edge control panel. The hardware architecture, illustrated in Figure 5, consists of a programmable logic controller (PLC), an industrial PC (IPC), and a gateway device.

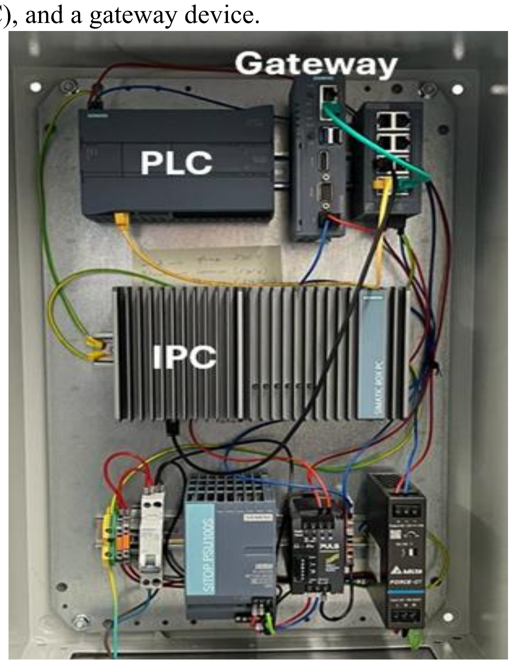

Figure 5:Hardware components of the BMS-integrated edge control architecture considered for Koopman–MPC deployment

The PLC acts as the primary interface with the physical AHU and the BMS. It is responsible for acquiring real-time measurements, enforcing actuator limits and safety logic, and applying control setpoints to the AHU actuators. In the proposed architecture, the PLC retains full authority over final actuation, ensuring safe operation regardless of the control strategy used at higher levels.
The IPC is intended to host the Koopman–MPC algorithm. Its computational resources are sufficient to perform lifted-state prediction and constrained optimization within the control sampling interval considered in this study.
The gateway device enables standardized communication between the PLC, IPC, and supervisory systems. It supports protocol translation between field-level communication (e.g., Modbus) and higher-level interfaces such as OPC UA, facilitating data exchange with the BMS.

Data flow and control integration

The data flow between the AHU, edge devices, and BMS is illustrated in Figure 6. At each sampling interval, the PLC acquires measurements from the AHU and relevant BMS controllers and makes them available to the IPC through the gateway. These measurements constitute the input to the Koopman–MPC algorithm, together with reference setpoints defined at the BMS level.
Based on the received measurements, the IPC executes the Koopman–MPC optimization using the EDMDc-identified linear predictor. The resulting control setpoints are transmitted back to the PLC, where they are evaluated against safety rules, actuator bounds, and operational constraints. If accepted, the setpoints are applied to the AHU actuators; otherwise, the PLC maintains the current operating point or falls back to standard BMS control logic.

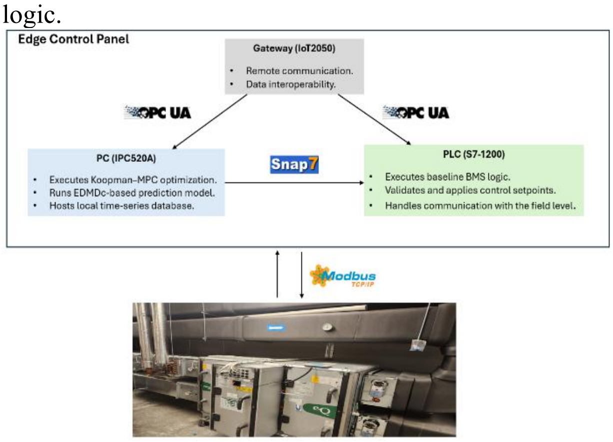

Figure 6:Edge Control Panel architecture used communication protocols for Koopman–MPC integration with the BMS

Conclusions

This paper proposed a data-driven Koopman–MPC framework for coordinated multi-input control of an AHU using operational BMS data. The approach identifies a finite-dimensional linear predictor in lifted space via EDMDc and embeds it in a constrained MPC formulation. The resulting controller targets supply air temperature and exhaust airflow while coordinating multiple AHU actuators within practical operating limits.

A high-fidelity NSS surrogate trained on measured data was used to evaluate closed-loop performance under realistic nonlinear AHU dynamics. The results indicate that the EDMDc-based Koopman predictor delivers stable short-horizon forecasts of the controlled outputs across representative operating conditions, enabling effective MPC-based regulation.

From a deployment perspective, the workflow is compatible with BMS-integrated edge execution. EDMDc identification and NSS training can be performed offline using historical BMS datasets, whereas online operation requires only state lifting, linear prediction, and constrained optimization at the BMS sampling interval. This separation reduces computational requirements and supports integration with standard automation hierarchies in which PLC-level logic enforces safety constraints and fallback operation.

Future work will focus on experimental validation on the real AHU, with the Koopman–MPC implemented as a supervisory layer in real time and benchmarked against the baseline BMS control. This will enable a quantitative assessment of comfort tracking, actuation behavior, and energy-related performance under comparable disturbance conditions.

Acknowledgements

This work was funded by the European Commission under Horizon Europe (Grant 101096789).

Nomenclature

AHU	Air-Handling Unit
BMS	Building Management System
DRL	Deep Reinforcement Learning
EDMDc	Extended Dynamic Mode Decomposition with Control
HVAC	Heating, Ventilation, and Air Conditioning
IPC	Industrial PC
LSTM	Long Short-Term Memory
MIMO	Multi-Input Multi-Output
MPC	Model Predictive Control
NSS	Neural State-Space
PID	Proportional–Integral–Derivative
PLC	Programmable Logic Controller

References

Afram, A. and Janabi-Sharifi, F. (2014) “Theory and applications of HVAC control systems – A review of model predictive control (MPC),” Building and Environment, 72, pp. 343–355. Available at: https://doi.org/10.1016/j.buildenv.2013.11.016.

Asvadi-Kermani, O. et al. (2022) “Energy Optimization of Air Handling Units Using Constrained Predictive Controllers Based on Dynamic Neural Networks,” IEEE Access, 10, pp. 56578–56590. Available at: https://doi.org/10.1109/ACCESS.2022.3177660.

Deshmukh, S., Glicksman, L. and Norford, L. (2020) “Case study results: Fault detection in air-handling units in buildings,” Adv. Build. Energy Res., 14(3), pp. 305–321. Available at: https://doi.org/10.1080/17512549.2018.1545143.

Matetić, I. et al. (2022) “A Review of Data-Driven Approaches and Techniques for Fault Detection and Diagnosis in HVAC Systems,” Sensors 2023, Vol. 23, 23(1). Available at: https://doi.org/10.3390/s23010001.

Taheri, S. et al. (2021) “Fault detection diagnostic for HVAC systems via deep learning algorithms,” Energy Build., 250, p. 111275. Available at: https://doi.org/10.1016/j.enbuild.2021.111275.

Wahba, N. et al. (2023) “Efficient HVAC system identification using Koopman operator and machine learning for thermal comfort optimisation,” Building and Environment, 242(1), p. 110567. Available at: https://doi.org/10.1016/j.buildenv.2023.110567.

Yue, B. et al. (2023) “Energy-oriented control retrofit for existing HVAC system adopting data-driven MPC – Methodology, implementation and field test,” Energy and Buildings, 295, p. 113286. Available at: https://doi.org/10.1016/j.enbuild.2023.113286.

Zawacki, C.C. and Abed, E.H. (2023) “Dynamic Mode Decomposition for Control Systems with Input Delays,” IFAC-PapersOnLine, 56(3), pp. 97–102. Available at: https://doi.org/10.1016/j.ifacol.2023.12.007.

Zheng, W., Wang, D. and Wang, Z. (2024) “Economic model predictive control for building HVAC system: A comparative analysis of model-based and data-driven approaches using the BOPTEST Framework,” Applied Energy, 374, p. 123969. Available at: https://doi.org/10.1016/j.apenergy.2024.123969.

Zou, Z., Yu, X. and Ergan, S. (2020) “Towards optimal control of air handling units using deep reinforcement learning and recurrent neural network,” Building and Environment, 168, p. 106535. Available at: https://doi.org/10.1016/j.buildenv.2019.106535.